Correction of NOAA-20 VIIRS Day/Night Band Low-Gain Stage Gain Calibration Errors by Scaling Factors Derived from Prelaunch Testing Data

Yalong Gu[a], Slawomir Blonski[a], Wenhui Wang[b], Taeyoung Choi[a], Sirish Uprety[b], Xi Shao[b], and Changyong Cao[c]

[a]Global Science & Technonlogy, Inc., Greenbelt, MD USA 20770

[b]Cooperative Institute for Satellite Earth System Studies (CISESS), Earth System Science Interdisciplinary Center, University of Maryland, College Park, MD, USA 20740

[c]Center for Satellite Application and Research, NESDIS/NOAA, College Park, MD USA 20740

ABSTRACT

The operational VIIRS Day/Night Band (DNB) Low Gain Stage (LGS) gain is calibrated by the onboard solar diffuser when it is fully illuminated by the Sun. Such calibration method relies on assumption of the same calibrator view and Earth view responses of the LGS. However, analysis of the NOAA-20 VIIRS DNB prelaunch testing data shows this assumption is not valid for all aggregation modes and detectors, consequently yielding striping in NOAA-20 VIIRS DNB daytime images collected by its LGS. Through applying scaling factors derived from the prelaunch testing data, the operational LGS gain calibration errors are corrected and striping in the reprocessed DNB daytime images is reduced.

Keywords: Radiometric calibration, gain, striping

1. INTRODUCTION

Day/Night Band (DNB) is a panchromatic visible and near-infrared band of the Visible Infrared Imaging Radiometer Suite (VIIRS) on-board the Suomi National Polar-orbiting Partnership (Suomi-NPP) and NOAA-20 satellites. It is composed of three independent bands, namely Low-Gain Stage (LGS), Mid-Gain Stage (MGS), and High-Gain Stage (HGS), designed to observe the Earth during daytime (LGS), twilight (MGS) and nighttime (HGS), respectively. After automatic selection of the gain stage, DNB is able to produce imagery of the Earth during both day and night with the radiance range from 3×10^{-9} W·cm^{-2}·sr^{-1} to 2×10^{-2} W·cm^{-2}·sr^{-1} [1][2].

The three gain stage design and the large dynamic range make the radiometric calibration of DNB very complicated. Only the LGS can be calibrated by the sunlight via the onboard solar diffuser. The MGS and HGS are calibrated indirectly, through transferring the LGS gain by multiplying the gain ratios of MGS/LGS and HGS/MGS evaluated in the twilight region. Although the requirement of DNB's radiometric calibration is rather loose, which is from 5% for the LGS to 100% for the HGS [3], high quality of DNB imagery is demanded. However, complicated radiometric calibration process brings artifacts (mostly striping) to the calibrated DNB images, degrading their quality.

Since the launch of Suomi-NPP in October 2011, striping has appeared in its VIIRS DNB imagery from both day and night scenes. For example, up to 42% of a daytime scene output by the LGS is affected by striping [4]. It was discovered that residual stray light, HAM side difference, electronic effects, and detector nonlinearity are major causes of the striping [5]. An algorithm based on the histogram matching method was developed to de-stripe all scenes, especially imagery in the twilight regions where scene illumination changes rapidly over short distances [5]. Recent efforts devoted to stray light correction also led to two updated methods, namely automatic stray light correction based on light contamination ranking index [6] and time-dependent stray light correction [7].

The second VIIRS DNB onboard NOAA-20 has been deployed in space for operation since the launch of the satellite in November 2017. A significant difference compared to the DNB onboard Suomi-NPP is the special aggregation option known as Option 21 which is for mitigating detector nonlinearity at high scan angles found during the prelaunch testing [3][8]. Option 21 extends aggregation mode 21 up to the edge of scan (in place of the modes 22 to 32) [9]. It was expected that striping in the NOAA-20 VIIRS DNB imagery would be smaller than for Suomi-NPP as high aggregation zones are more susceptible to striping. However, striping appears in NOAA-20 VIIRS DNB imagery as well, both in daytime and

Earth Observing Systems XXV, edited by James J. Butler, Xiaoxiong (Jack) Xiong, Xingfa Gu, Proceedings of SPIE Vol. 11501, 115010Y · © 2020 SPIE
CCC code: 0277-786X/20/$21 · doi: 10.1117/12.2568783

nighttime. Severe striping in NOAA-20 VIIRS DNB nighttime imagery, in particular in aggregation zone 21, which occupies about 30% of a DNB image, has been addressed by updating the algorithm for the gain ratios determination [10].

In this paper, we focus on a striping correction for the NOAA-20 VIIRS DNB daytime imagery. Operational VIIRS DNB LGS gain is calibrated by an onboard solar diffuser when it is fully illuminated by the Sun, relying on the assumption of the same LGS responses in the calibrator view and the Earth view. Our analysis of NOAA-20 VIIRS DNB prelaunch testing data shows that this assumption is not valid for all aggregation modes and detectors, consequently yielding striping in NOAA-20 VIIRS DNB daytime images collected by its LGS. Through applying scaling factors derived from the prelaunch testing data, the operational LGS gain calibration errors are corrected and striping in the reprocessed DNB daytime images is reduced.

2. ANALYSIS OF DAYTIME IMAGES AFFECTED BY STRIPING

On orbit, DNB, as well as other VIIRS bands, observes the Earth through the Earth view (EV) port of VIIRS in a scanning manner, by a rotating telescope and the half-angle mirror (HAM) [11]. The entire swath width of an EV scan is about 3000 kilometers. In order to eliminate the bow-tie effect and keep a constant ground resolution across a scan, the whole EV is divided into certain aggregation zones on each side of the nadir where a different number of detectors is grouped according to the specific aggregation mode [12]. After aggregation, the size of a single-scan DNB EV data is 16 × 4064 (track × scan). The 16 along-track pixels are created by on-board aggregation of 672 along-track detectors. Unless otherwise specified, the actual detectors are named as "subpixels", while the term "detector" used in the rest of the paper refers to 16 virtual along-track detectors, following the VIIRS nomenclature [11]. In operation, every 48 consecutive scans of the Earth are stitched together to form an Earth image, known as a granule whose size is 768 pixels × 4064 pixels (track × scan).

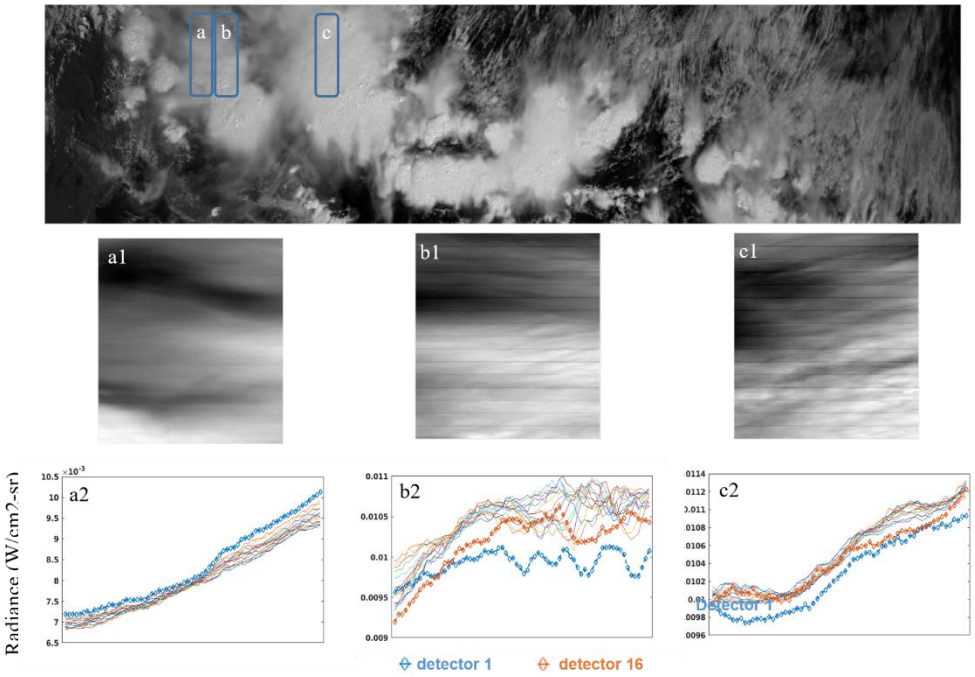

Figure 1. NOAA-20 VIIRS DNB nighttime image observed at 19:06 UTC on July 21, 2019. (a1), (b1) and (c1) are the zoom-in images of the circled regions (a) (b) and (c) respectively. (a2), (b2) and (c2) are the detectors' radiances of a scan shown in (a1), (b1) and (c1) respectively.

Deep convective clouds (DCCs) are extremely cold clouds abundant over tropical areas. Because of their persistence, they are ideal targets for monitoring calibration stability of spaceborne radiometers on orbit [13][14]. The large size and high brightness also make DCCs favorable targets for evaluating quality of DNB imagery. Figure 1 shows a daytime image of DCCs observed by NOAA-20 VIIRS DNB at 19:06 UTC on July 21, 2019. In general, the observed DCCs are relatively uniform, for example the DCCs in the center of the image. However, striping can be seen in the recorded DCCs in the left

side of the image, as illustrated by Figures 1a, 1b and 1c. The strips are either bright in aggregation zone 17 (Figure 1, a1 and a2) or dark in aggregation zone 9 (Figure 1, b1 and b2) and 16 (Figure 1, c1 and c2).

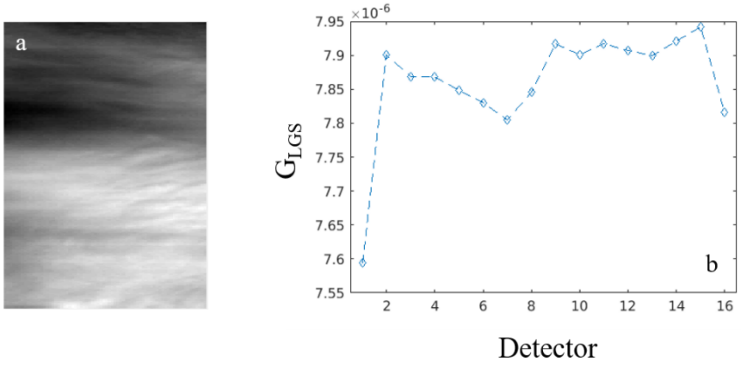

Figure 2. (a) The dark offset and RVS correct DN image of Figure 1 b1 (aggregation zone 16). (b) LGS calibration coefficients of all detectors for aggregation zone 16.

The striping pattern caused by certain detectors suggests incorrected calibration of these detectors. The LGS, which is responsible for the daytime observations of the Earth, is calibrated by a linear equation,

$$L = G_{LGS} \times (DN - DN_0)/RVS, \tag{1}$$

where L denotes radiance, G_{LGS} is the LGS calibration coefficient determined with the onboard solar diffuser, DN is the raw measurement data, and DN_0 is the corresponding dark offset. RVS (Response Versus Scan) accounts for scan-angle dependency of the signal reflection from the HAM. Figure 2 shows the image of dark-offset corrected raw measurement $(DN - DN_0)/RVS$ of aggregation zone 16 corresponding to Figure 1b1 and the LGS gain. It can be clearly seen that the image of $(DN - DN_0)/RVS$ is free of striping while the LGS calibration coefficients of detectors 1 and 16 are smaller than their neighboring detectors by as much as 4%. The analysis of striping in aggregation zones 9 and 17 (Figure 1, a1 and c1) also confirms that the LGS calibration coefficients for detectors 1 and 16 (aggregation mode 9) and detector 1 (aggregation mode 17) are different from their neighboring detectors. Therefore, we determined that the LGS calibration coefficients are the cause of striping show in Figures 1.

3. ON-ORBIT AND PRELAUNCH DNB LGS GAIN CALIBRATION BY SOLAR DIFFUSER

The operational VIIRS DNB LGS gain is calibrated by its onboard solar diffuser (SD) when it is fully illuminated by sunlight,

$$G_{LGS} = \frac{L_{SD}}{dn_{SD}} \tag{2}$$

where dn_{SD} is the dark offset corrected LGS response when it views the SD in unit of digital number. L_{SD} is the expected solar radiance reflected by the SD within the spectral range of the LGS [11],

$$L_{SD} = \int H \cdot RSR \cdot RVS_{SD} \cdot \Phi_{sun} \cdot BRDF \cdot \tau_{SDS} \cdot \frac{\cos(\theta_{inc})}{4\pi d^2} d\lambda, \tag{3}$$

where H is the so-called H factor that characterizes the SD degradation. RSR is the relative spectral response function of the LGS. RVS_{SD} is the RVS at the scan angle of the SD view. BRDF is the bidirectional reflectance distribution function of the SD. τ_{SAS} is the spectral transmission function of the screen in front of the SD. Φ_{sun} is the spectral irradiance (flux) of the Sun. θinc is the incidence angle of sunlight on the SD. d is the distance between Earth and the Sun. The LGS gain is calibrated per detector, HAM side and aggregation mode. The calibration coefficients that are derived via the SD are then used to convert the raw measurements of the Earth to radiances according to Eq. 1. Such calibration process relies on an assumption of the same DNB LGS EV and SD responses to the same incident light. However, it is known that the DNB

electronic timing is different in the calibrator sectors that include the SD view versus the EV portion [11]. As shown in Figure 1, striping only appears in certain aggregation zones. This suggests that the above-mentioned assumption is not valid for all detectors and aggregation modes of the LGS.

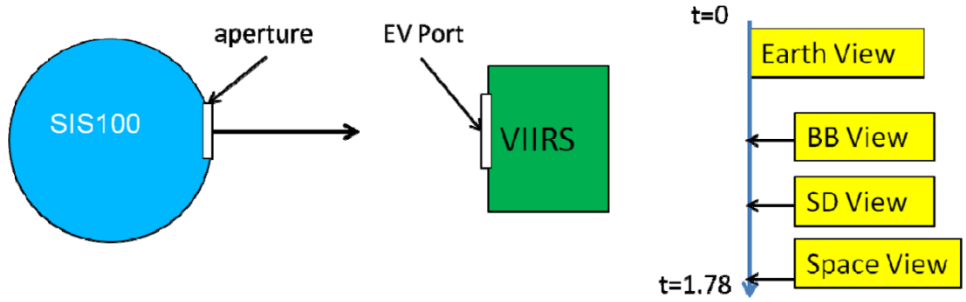

Figure 3. Illustration setup for NOAA-20 VIIRS prelaunch radiometric testing. After Figure 2 in Ref [8].

Investigating whether the DNB LGS EV and SD respond similarly requires illumination by the same light source whose spectral radiance is well characterized. NOAA-20 (named as JPSS-1 before launch) VIIRS DNB has been thoroughly characterized through prelaunch testing [3]. During the testing, the EV port of the VIIRS was illuminated by a special integrating sphere known as SIS100, illustrated by Figure 3 [8]. By locking the telescope at the direction toward the aperture of SIS100, VIIRS collected the EV, blackbody (BB), SD, and space view (SV) data, in sequence.

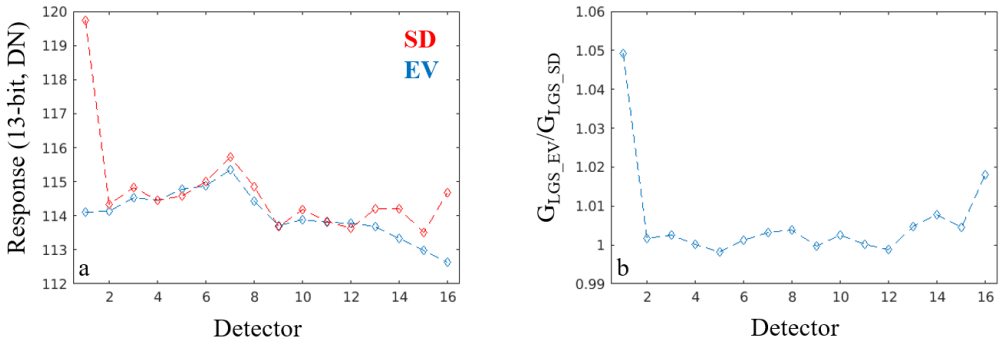

Figure 4. (a) DNB responses (dn_{EV} and dn_{SD}) to the selected light level in the prelaunch testing. (b) Ratio of the EV and SD gains for each detector (aggregation mode 16 and HAM side A).

The radiometric test was performed at several discrete light levels to cover the whole dynamic range of the LGS. The spectral radiance at each light level was measured with a spectroradiometer and a NIST-traceable FEL standard irradiance lamp [3].In order to simulate the condition of on-orbit LGS calibration, we selected a light level whose total radiance in the spectral range of the LGS is similar to the in-band solar radiance when the LGS is calibrated on-orbit. The prelaunch EV and SD LGS gains are evaluated by the following equation, similar to Eq. 2:

$$G_{LGS\_EV} = \frac{L_{SIS}}{dn_{EV}} \tag{4a}$$

$$G_{LGS\_SD} = \frac{L_{SIS}}{dn_{SD}} \tag{4b}$$

where L_{SIS} is the source radiance in the spectral range of the LGS for the selected light level. dn_{EV} and dn_{SD} are offset corrected EV and SD responses. SIS100 monitoring data show that the prelaunch testing satisfies the requirement of the same illumination for both the EV and the SD. Figure 4(a) shows the EV and SD responses for all detectors of aggregation mode 16 for the selected light level. It can be seen that the EV responses of detectors 1 and 16 are smaller than their SD counterparts. Consequently, the EV LGS calibration coefficients are underestimated by the SD LGS response measurements. These results confirm that the assumption of the same EV and SD responses of NOAA-20 VIIRS DNB LGS is not valid for aggregation mode 16. Our analysis of aggregation modes 9 and 17 using the same prelaunch testing data also led to the same conclusion.

In Ref. [15], it is pointed out that the spectral shape of SIS100 differs from the solar spectrum. Such mismatch probably yields non-negligible uncertainties in the absolute prelaunch gain calibration because of the DNB broad spectral response. We also noted that the LGS SD response to the selected light level of the prelaunch testing (shown in Figure 4a) is different from the SD response when it is illuminated by the Sun on orbit while the in-band radiance is similar. However, our concerned quantity is the relative ratio between the EV and SD LGS gains for different detectors. The uncertainty in the derived ratio is considered negligible despite of the source difference.

4. STRIPING CORRECTION BY RESCALED LGS GAIN

Our analysis of the NOAA-20 VIIRS DNB prelaunch testing data in Sec. 3 shows that the LGS gain derived by the SD data differs from the EV counterparts for certain detectors and aggregation modes. Such difference induces striping in the operational NOAA-20 VIIRS DNB daytime imagery which is calibrated by the LGS gain determined by the SD data. We propose a solution for correcting such kind of striping by scaling the operational LGS calibration coefficient with a factor derived from the NOAA-20 VIIRS DNB prelaunch testing data:

$$G_{LGS\_c} = s_{prelaunch} \times G_{LGS} \tag{5}$$

where G_{LGS} is the operational LGS calibration coefficient defined in Eq. 2. The scaling factor $s_{prelaunch}$ is the ratio of the prelaunch EV and SD LGS gains defined in Eqs. 4:

$$s_{prelaunch} = G_{LGS\_EV}/G_{LGS\_SD} \tag{6}$$

Figure 5 shows the radiance images of aggregation zones 9, 16 and 17 of the granule collected at 19:06 UTC on July 20, 2019, which were reprocessed using the corrected LGS calibration coefficients G_{LGS_C}. It can be clearly seen that the striping, which is visible in Figures 1 a1, b1 and c1, disappears in Figure 5. Successful correction of striping in operational NOAA-20 VIIRS DNB daytime imagery by the scaling factor derived from the prelaunch testing data also suggests negligible uncertainty in the scaling factor due to the spectral different between SIS100 and the Sun, as discussed at the end of Sec. 3.

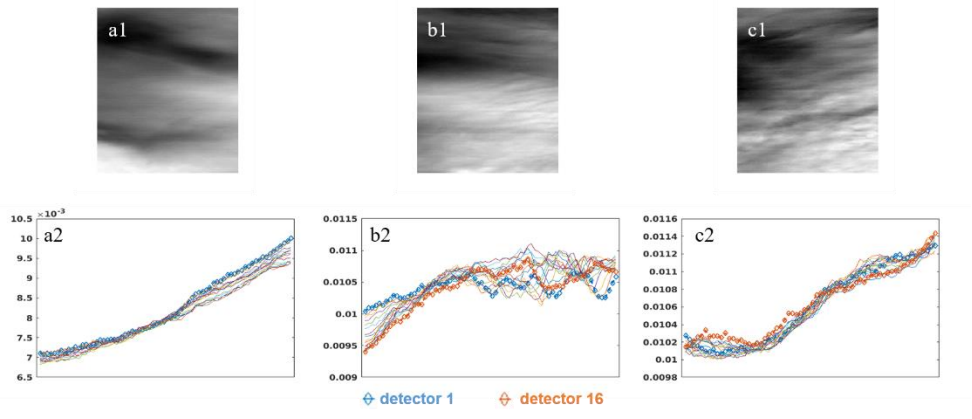

Figure 5. (a1) Recalibrated NOAA-20 VIIRS DNB daytime radiance image of aggregation zone 17 shown in Figure 1 a1. (a2) Recalibrated detectors' radiances of the scan shown in Figure 1 a2. (b1) Recalibrated NOAA-20 VIIRS DNB daytime

radiance image of aggregation zone 16 shown in Figure 1 b1. (b2) Recalibrated detectors' radiances of the scan shown in Figure 1 b2. (c1) Recalibrated NOAA-20 VIIRS DNB daytime radiance image of aggregation zone 9 shown in Figure 1 c1. (c2) Recalibrated detectors' radiances of the scan shown in Figure 1 c2.

Figure 5 demonstrates that striping in certain aggregation zones of operational NOAA-20 VIIRS DNB daytime images can be successfully corrected by the scaling factor derived from the prelaunch testing data. It is curious to ask if such correction of operational LGS gain is necessary for all 21 aggregation modes of NOAA-20 VIIRS DNB LGS. Figure 6 shows the ratio of the prelaunch EV and SD LGS gain for the aggregation modes of NOAA-20 VIIRS DNB. While the relative difference between two versions of LGS gains is less than 1% for many detectors and aggregation modes, there are a few detectors and aggregation modes exhibiting non-negligible values, for example detector 7 of aggregation mode 14. However, unlike aggregation zones 9, 16 and 17, clear striping is not observed in these aggregation zones of operational NOAA-20 VIIRS DNB daytime imagery. Such phenomenon indicates complicated relation among prelaunch and postlaunch LGS gains for both the EV and SD. As our purpose is to correct striping observed in operational imagery, we recommend correction of operational LGS gains for the aggregation modes that show visible striping, for example aggregation modes 9, 16 and 17.

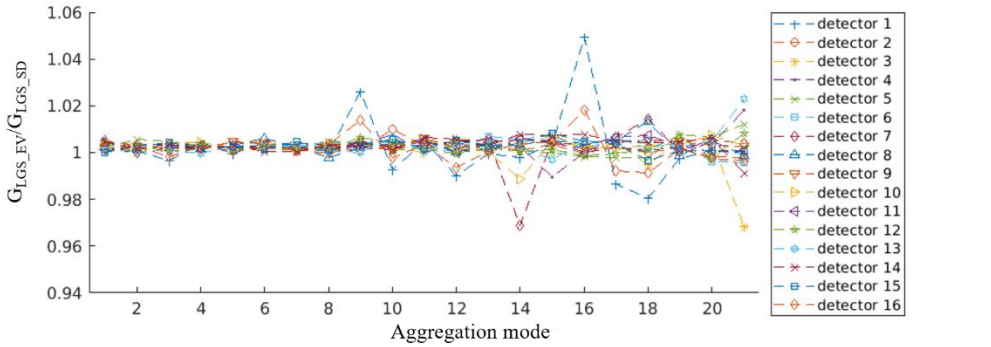

Figure 6. Ratio of the EV and SD LGS gains determined by the NOAA-20 VIIRS DNB prelaunch testing data for all operational aggregation modes.

5. CONCLUSIONS

In this paper, we have shown that striping observed in a few aggregation zones of operational NOAA-20 VIIRS DNB daytime imagery is due to discrepancy between the EV and SD LGS gains. Difference between two versions of the LGS gain is quantified through analysis of NOAA-20 VIIRS DNB prelaunch testing data. After correcting the operational LGS gain calibration errors by the derived scaling factor, striping in the reprocessed NOAA-20 VIIRS DNB daytime images is reduced.

It is worth noting that the ratio between the EV and SD LGS gains can only be evaluated by the prelaunch testing data. This is because it is impossible for the EV and SD to be illuminated by the same light source on orbit. However, it is known that a spaceborne radiometer is subject to gain degradation due to exposure in the space environment. Before applying the scaling factor derived from the NOAA-20 VIIRS DNB prelaunch testing data for the operational NOAA-20 VIIRS DNB LGS gain calibration, more analysis is needed to verify whether it works effectively for correcting striping in NOAA-20 VIIRS DNB daytime images collected since the launch of the satellite in November 2017.

ACKNOWLEDGMENT

This work is funded by the Joint Polar Satellite System program office. The manuscript contents are solely the opinions of the authors and do not constitute a statement of policy, decision, or position on behalf of NOAA or the U.S. government.

REFERENCES

[1] Cao, C., Xiong, J., Blonski, S., Liu, Q., Uprety, S., Shao, X., Bai, Y., and Weng, F., "Suomi NPP VIIRS sensor data record verification, validation, and long-term performance monitoring," J. Geophys. Res. **118**, 11644-11678 (2013).

[2] Liao, L. B., Weiss, S., Mills, S., and Hauss, B., "Suomi NPP VIIRS day-night band on-orbit performance," J. Geophys Res. **118**, 12705-12718 (2013).

[3] Schwarting, T., McIntire, J., Oudrari, H., and Xiong, X., "JPSS-1/NOAA-20 VIIRS Day-Night Band prelaunch radiometric calibration and performance," IEEE Trans. Geosci. Remote Sens. **57**, 7534-7546 (2019).

[4] Mills, S., and Miller, S. D., "VIIRS Day-Night Band calibration methods for improved uniformity," Proc. SPIE **9218**, 921809 (2014).

[5] Mills, S, and Miller, S., "VIIRS Day/Night Band – correcting striping and nonuniformity over a very large dynamic range," J. Imaging **2**, 9 (2016).

[6] Shao, X., Liu, T., Uprety, S., Wang, W., Zhang, B., and Cao, C., "A light contamination ranking index-based method for automating VIIRS Day/Night Band stray light correction," Proc. SPIE **10764**, 107641I (2018).

[7] Sun, C., Schwarting, T., Geng, X., Chiang, K., Chen, H., and Xiong, X., "VIIRS DNB time-dependent stray light correction," Proc. SPIE **11271**, 11271W (2019).

[8] Lee, S., Wang, W., and Cao, C., "JPSS-1 VIIRS DNB nonlinearity and its impact on SDR calibration," Proc. SPIE **9607**, 960717 (2015).

[9] Wang, W. and Cao, C., "NOAA-20 VIIRS DNB Aggregation Mode Change: Prelaunch Efforts and On-Orbit Verification/Validation Results," IEEE J Sel Top Appl Earth Obs Remote Sens. **12**, 2015-2023 (2019).

[10] Gu, Y., Uprety, S., Blonski, S., Shao, X., and Cao, C., "Correction of detector nonlinearity induced striping in VIIRS Day/Night Band nighttime imagery," Proc. SPIE **11271**, 11271T (2019).

[11] Joint Polar Satellite Systems VIIRS Radiometric Calibration Algorithm Theoretical Basis Document, Revision D, https://www.star.nesdis.noaa.gov/jpss/documents/ATBD/D0001-M01-S01-003_JPSS_ATBD_VIIRS-SDR_D.pdf (2017).

[12] Joint Polar Satellite System VIIRS Geolocation Algorithm Theoretical Basis Document, Revision A, https://www.star.nesdis.noaa.gov/jpss/documents/ATBD/D0001-M01-S01-004_JPSS_ATBD_VIIRS-Geolocation.pdf (2017).

[13] Wang, W., and Cao, C., "Monitoring the NOAA operational VIIRS RSB and DNB calibration stability using monthly and semi-monthly deep convective clouds time series," Remote Sens **8**, 32 (2016).

[14] Cao, C., Bai, Y., Wang, W., and Choi, T., "Radiometric inter-consistency of VIIRS DNB on Suomi NPP and NOAA-20 from observations of reflected lunar lights over deep convective clouds," Remote Sens **11**, 934 (2019).

[15] Xiong, X. and Butler, J., "Challenges and approaches for sensor reflective solar calibration," IEEE International Geoscience and Remote Sensing Symposium (IGARSS), Yokohama, Japan, July 2019, 5796 – 5799.